ACS APPLIED MATERIALS & INTERFACES

Research Article

www.acsami.org

Performance Enhancement of Dye-Sensitized Solar Cells Using an Ester-Functionalized Imidazolium Iodide as the Solid State Electrolyte

Xin Xu, Hong Wang, Feng Gong, Gang Zhou, and Zhong-Sheng Wang*

Department of Chemistry, Lab of Advanced Materials, Fudan University, 2205 Songhu Road, Shanghai 200438, P. R. China

ABSTRACT: Linking an ester group to the imidazolium ring has been demonstrated to improve solar cell performance in terms of short-circuit photocurrent (J_{sc}), open-circuit photovoltage (V_{oc}), and fill factor (FF) in particular, when the imidazolium iodide mixed with iodine and LiI is used as a solid state electrolyte of dye-sensitized solar cells. Herein, the effect of ester group on solar cell performance has been investigated by means of intensity modulated photocurrent/photovoltage and electrochemical impedance spectroscopy. From the alkyl- to ester-functionalized imidazolium iodide, the increase in J_{sc} is attributed to the increased charge collection efficiency due to the enhanced conductivity, the increase in V_{oc} is caused by the upward shift of conduction band edge of TiO_2, which compensates for the voltage loss arising from the higher charge recombination rate, and the remarkable increase in FF is attributed to the decreased series resistance along with the increased V_{oc} and decreased diode quality factor.

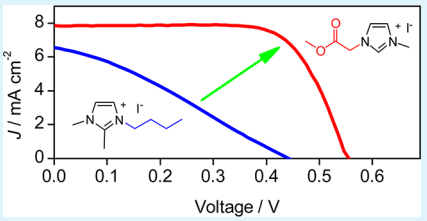

KEYWORDS: *imidazolium iodide, ester group, electrochemical impedance, charge collection efficiency, dye-sensitized solar cell*

INTRODUCTION

Dye-sensitized solar cells (DSSCs) as next generation promising photovoltaic devices have attracted increasing scientific interest since the milestone report by Grätzel's group.[1] Owing to their low fabrication cost, simple manufacturing process, and high theoretical efficiency, they were thought of as promising alternatives to the traditional Si based solar cells. Over the past two decades, great attention has been paid to DSSCs and remarkable efforts have been made to develop new materials for efficient DSSCs.[2−7] Hitherto, the power conversion efficiency has been raised up to 12.3% with a volatile organic solvent based electrolyte.[8] However, the use of volatile liquid electrolytes limits the practical application of DSSCs, as the disadvantages of leakage and volatilization reduce the device's long-term stability. For this reason, solid state electrolytes have been developed and employed to construct solid state DSSCs (ssDSSCs).[9−11]

Solid state imidazolium iodide salts have been demonstrated to be promising materials as solid state electrolytes for ssDSSCs.[12,13] Recently, we designed and synthesized a solid state ester-functionalized imidazolium iodide (1-(2-methoxy-2-oxylethyl)-3-methyl imidazolium iodide, EMImI, Figure 1) for use in ssDSSCs, which yielded power conversion efficiency as high as 6.63% under illumination of AM 1.5 G simulated solar light (100 mW cm^{-2}) and exhibited very good long-term stability under 1 sun soaking.[14] As compared to the alkyl-substituted imidazolium iodide (1,2-dimethyl-3-*n*-propyl-imidazolium iodide, DMPImI, Figure 1), the introduction of an ester group to the imidazolium ring improves all photovoltaic performance parameters significantly. However, the mechanism by which the ester group influences solar cell performance is not clear to date. To develop more efficient imidazolium based ionic conductors, it is necessary to clarify the effect of the ester group on solar cell performance.

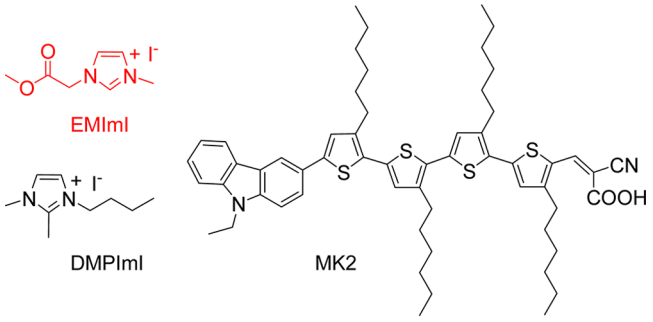

Figure 1. Structures of ionic conductors (EMImI, DMPImI) and the dye MK2.

Herein, we present the intensity-modulated photocurrent/photovoltage spectroscopy (IMPS/IMVS) and electrochemical impedance spectroscopy (EIS) study on ssDSSCs based on EMImI and DMPImI, respectively. It was found that the ester group improved the charge collection efficiency, reduced the series resistance, and shifted the conduction band (CB) edge of TiO_2 upward. As a consequence, solar cell performance was improved remarkably by the introduction of an ester group to the imidazolium ring.

Received: January 18, 2013
Accepted: March 19, 2013
Published: March 19, 2013

   dx.doi.org/10.1021/am4002293 | *ACS Appl. Mater. Interfaces* 2013, 5, 3219−3223

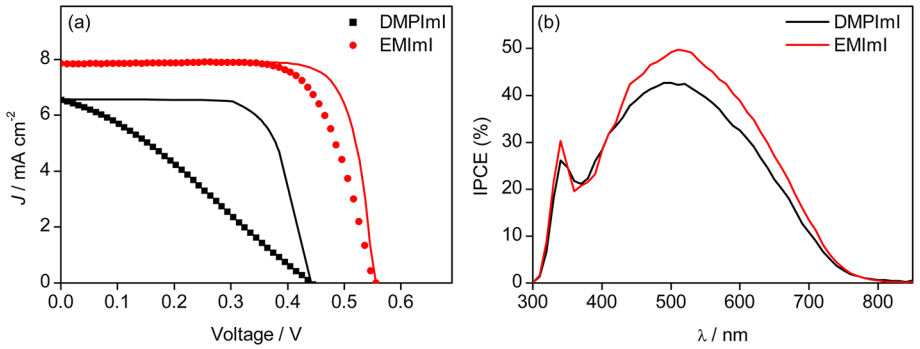

Figure 2. (a) $J-V$ curves for ssDSSCs with EMImI or DMPImI based solid electrolyte containing I_2 and LiI. The line curves (the black line for DMPImI and the red line for EMImI) are obtained by correcting the potential drop at the total series resistance. (b) IPCE spectra for the above cells.

EXPERIMENTAL SECTION

Materials and Reagents. EMImI and DMPImI were available from our previous study.[14] The organic dye (MK2, Figure 1) was prepared according to a literature method.[15,16] LiI and I_2 were obtained from Acros. A mixture of EMImI (or DMPImI) with iodine and LiI (the molar ratio of EMImI or DMPImI/I_2/LiI = 5/1/1.25) was employed as the solid state electrolyte for ssDSSCs. It is noted that each component in the electrolyte is solid and the mixture is solid too. Transparent conductive glass (F-doped SnO_2, FTO, 15 Ω/square, transmittance of 85%, Nippon Sheet Glass Co., Japan) was used as the substrate for the fabrication of TiO_2 thin film electrode.

Fabrication of ssDSSCs. TiO_2 films (~4.5 μm) composed of ~20 nm TiO_2 nanoparticles[17] were fabricated on FTO substrates with a screen printing method. After the films were sintered at 500 °C for 2 h, they were treated with 0.05 M $TiCl_4$ aqueous solution at 70 °C for 30 min followed by washing with deionized water and heating at 450 °C for 30 min. When TiO_2 electrodes were cooled down to ~120 °C, they were immersed in the MK2 dye solution (0.3 mM in toluene) for 24 h at room temperature for complete dye adsorption. The dye-loaded TiO_2 film as working electrode and the Pt-deposited FTO as counter electrode were separated by a hot-melt Surlyn film (30 μm) and sealed together by pressing them under heat. The methanol solution of the solid electrolyte was injected repeatedly into the interspace between the working and counter electrodes from the two holes predrilled on the back of the counter electrode and dried on a hot plate with the temperature of 50 °C until the TiO_2 porous film was filled with solid state electrolyte. The cell was further dried in a vacuum oven at 50 °C for 2 days to remove the residue methanol. Finally, the two holes were sealed with a Surlyn film covered with a thin glass slide under heat.

Photovoltaic Measurements. The working performance of DSSCs were evaluated by recording the $J-V$ curves with a Keithley 2400 source meter under the illumination of AM 1.5 G simulated solar light coming from a solar simulator (Oriel-91193 equipped with a 1000 W Xe lamp and an AM 1.5 filter). The incident light intensity was calibrated using a reference Si solar cell (Oriel-91150). Action spectra of incident monochromatic photon-to-electron conversion efficiency (IPCE) as a function of wavelength were obtained with an Oriel-74125 system. The intensity of incident monochromatic light was measured with a Si detector (Oriel-71640). To eliminate the stray light, a black mask with an aperture area of 0.2304 cm^2, measured with a Nikon Digital Camera controlled by a computer using an objective micrometer ruler as a reference, was used to cover the devices during measurements.

Characterizations. The thickness of the films was determined with a surface profiler (Dektak 150, Veeco). IMPS, IMVS, and EIS were carried out with an electrochemical workstation (Zahner XPOT, Germany) in combination with a green light emitting diode (LED, 532 nm) and a control system. The conductivity of the solid state electrolytes, which were sandwiched between two identical Pt electrodes, was determined by EIS under dark in a frequency range of 1 Hz to 1 MHz. EIS for ssDSSCs under illumination of green light (532 nm, various intensities) was measured at open-circuit and 10 mV ac amplitude in a frequency range of 0.1 Hz–1 MHz at room temperature. The IMPS and IMVS were recorded at room temperature with light (532 nm) intensity ranging from 10 to 45 W m^{-2}, in modulation frequency ranging from 0.1 Hz to 10 kHz and modulation amplitude less than 5% of the light intensity.

RESULTS AND DISCUSSION

Photovoltaic Performance. Figure 2a shows the $J-V$ curves for the ssDSSCs based on the two solid state electrolytes under illumination of simulated AM 1.5 G solar light (100 mW cm^{-2}) with the corresponding data summarized in Table 1. The

Table 1. Photovoltaic, Energetic, and Recombination Parameters[a]

	DMPImI	EMImI
J_{sc}/mA cm^{-2}	6.56	7.86
V_{oc}/mV	442	556
FF	0.30	0.71
η/%	0.87	3.10
calculated FF	0.70	0.79
internal FF	0.71	0.79
$E_c - E_{redox}$/eV	0.76	0.97
J_0/mA cm^{-2}	1.8×10^{-4}	3.3×10^{-7}
J_{0k}/mA cm^{-2}	4.0×10^{4}	2.0×10^{6}
β	0.65	0.78

[a]The calculated FF is obtained from eq 6, and the internal FF is obtained by subtracting the potential drop at the series resistance.

alkyl-substituted imidazolium iodide (DMPImI) produced short-circuit photocurrent density (J_{sc}) of 6.56 mA cm^{-2}, open-circuit photovoltage (V_{oc}) of 442 mV, and fill factor (FF) of 0.30, corresponding to power conversion efficiency (η) of 0.87%. For EMImI, the ssDSSC yielded J_{sc} of 7.86 mA cm^{-2}, V_{oc} of 556 mV, and FF of 0.71, corresponding to η of 3.10%. When the ester group was attached to the imidazolium ring, J_{sc}, V_{oc}, and FF were improved by 20%, 26%, and 137%, respectively, resulting in an increase in η by 256%. Evidently, the ester group plays an important role in improving solar cell performance. Figure 2b displays the IPCE spectra for the above ssDSSCs. The low IPCE is attributed to the insufficient dye loading on thin films (4.5 μm). Compared to DMPImI, EMImI exhibited higher IPCE values in the spectral range of 420–750 nm. This accounts for the larger J_{sc} for the EMImI based ssDSSC.

Effect on J_{sc}. The J_{sc} is determined by light harvesting efficiency, electron injection efficiency, and charge collection efficiency. As the same dye and identical TiO_2 were used in this

study, light harvesting efficiency should be the same for the devices investigated. Therefore, the J_{sc} is determined by the electron injection efficiency and charge collection efficiency, which can be influenced by the CB edge (E_c) of TiO_2 and the conductivity of solid electrolyte, respectively. The relative CB edge can be derived from the relationship between chemical capacitance (C_μ) and quasi-Fermi level voltage (V_F), as shown in eq 1:[18]

$$C_\mu = \frac{q^2 N_L}{K_B T_0} \exp\left(\frac{qV_F + E_{redox} - E_C}{K_B T_0}\right) \quad (1)$$

where q is the elementary charge, N_L (= 10^{20} cm^{-3}) is the total density of band gap states,[18] K_B is the Boltzmann constant, T_0 is a parameter,[19] E_{redox} is the potential of redox species, and V_F is the bias voltage applied to the film in EIS measurement. Figure 3 shows the plot of chemical capacitance against voltage

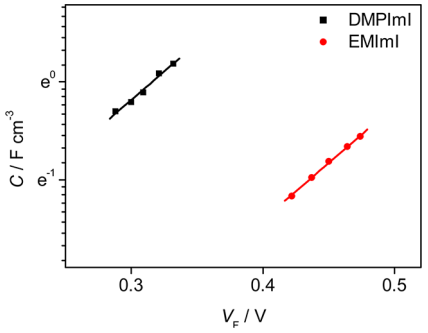

Figure 3. Chemical capacitance as a function of potential. The solid lines are fittings to eq 1.

obtained from EIS, from which the relative CB edge is determined (Table 1). The slopes are nearly the same for the two electrolytes, from which T_0 is determined to be 993 K.[19] At a fixed capacitance, a higher voltage indicates an upward displacement of the CB edge, while a lower voltage means a downward movement of the CB edge. It is derived from Figure 3 that the CB edge of TiO_2 in contact with EMImI is higher than that in contact with DMPImI by 205 mV.

The CB edge position is sensitive to the surface concentration of cations. In the case of EMImI, the strong interaction of carbonyl groups with Li^+ ions reduces the adsorption of Li^+ ions onto the TiO_2 surface.[14] As the CB edge shifts positively with increasing the surface concentration of Li^+ ions,[20] it is reasonable that the CB edge of TiO_2 in contact with EMImI is higher than that of TiO_2 in contact with DMPImI. When the CB edge is lowered, electron injection becomes facilitated and J_{sc} should increase. However, J_{sc} for EMImI is larger than that for DMPImI. As the lowest unoccupied molecular orbital (LUMO) of MK2,[15,16] which is 1.29 V higher than the redox potential of I^-/I_3^-, is 0.32 and 0.53 V (Table 1) higher than the CB edge of TiO_2 in contact with EMImI and DMPImI, respectively, it is reasonable to assume unity electron injection yield for both cases because the driving force (>0.3 eV) for electron injection is sufficiently high. Therefore, the difference of J_{sc} should be attributed to different charge collection efficiency, which is associated with the conductivity of solid state electrolyte. The conductivity was measured to be 0.19 and 4.03 mS cm^{-1} for DMPImI and EMImI, respectively. As EMImI has an ordered three-dimensional channel for iodide, it has a much higher conductivity than DMPImI as claimed in our previous report.[14] High conductivity favors electron transfer from the counter electrode to the electrolyte, and it is thus expected that charge collection efficiency can be improved with increasing the conductivity of the electrolyte.

Charge collection efficiency (η_{cce}) can be determined by the following equation:[21]

$$\eta_{cce} = 1 - \frac{\tau_d}{\tau_n} \quad (2)$$

where τ_d is the time constant that can be extracted from IMPS at short circuit and τ_n is the electron lifetime that can be extracted from IMVS at open circuit. Figure 4 shows the charge

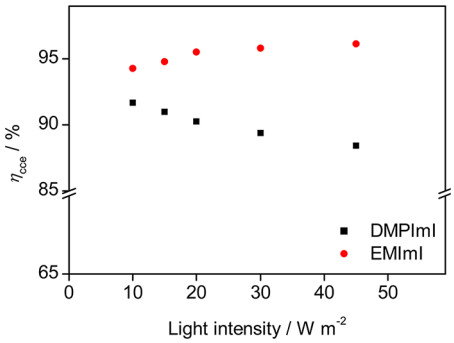

Figure 4. Charge collection efficiency at different light intensity (532 nm, LED light).

collection efficiency under green light (532 nm) illumination with different intensities. For EMImI, the charge collection efficiency is almost same (around 95%), indicating that charge collection is hardly limited by the conductivity of EMImI based solid state electrolyte. In contrast, the charge collection efficiency decreases with light intensity for DMPImI. This means that the charge collection efficiency is limited by the conductivity of DMPImI based solid state electrolyte. Under the same light intensity, the charge collection efficiency for EMImI is larger than that for DMPImI in the tested intensity range and the difference of charge collection efficiency becomes larger with increasing light intensity. It is concluded that the higher conductivity is responsible for the higher charge collection efficiency. Under illumination of LED green light (532 nm, 45 W cm^{-2}), the increase in J_{sc} (8.7%) is in good agreement with the increase in charge collection efficiency (7.6%). This agreement indicates that the difference of J_{sc} is attributed to the difference of charge collection efficiency, which originates from the different conductivity.

Recently, Bertoluzzi et al. pointed out that eq 2 should be valid only under the conditions that the cell active layer is thin enough so that the photogenerated electrons could either recombine with acceptors or be immediately collected to contribute to J_{sc}.[22] The calculation error from eq 2 becomes more prominent as the diffusion length decreases with regard to the active layer thickness. Therefore, to estimate charge collection efficiency more accurately, one should adopt the recently reported expressions taking linear or nonlinear charge recombination into account.[22]

Effect on V_{oc}. According to the diode model, the open-circuit photovoltage can be expressed as

dx.doi.org/10.1021/am4002293 | ACS Appl. Mater. Interfaces 2013, 5, 3219−3223

$$V_{oc} = \frac{K_B T}{q\beta} \ln\left(\frac{J_{sc}}{J_0} + 1\right) \approx \frac{E_c - E_{redox}}{q} + \frac{K_B T}{q\beta} \ln\left(\frac{J_{sc}}{J_{0k}}\right) \quad (3)$$

where β is an exponent governing the recombination, J_0 determines the dark current, J_{0k} determines the recombination rate, T (= 298 K here) is the temperature, and

$$J_0 = J_{0k} \exp\left(\frac{-\beta(E_c - E_{redox})}{K_B T}\right) \quad (4)$$

For a DSSC at a fixed temperature, the V_{oc} is determined by J_{sc}, J_0, and β or determined by J_{sc}, E_c, J_{0k}, and β. J_{sc} can be read from the $J-V$ curve under illumination while the relative E_c level can be obtained from the plot of chemical capacitance against potential (Figure 3). Evidently, a higher CB edge and slower charge recombination rate are favorable for higher V_{oc}. J_0, J_{0k}, and β can be derived from the plot of charge recombination resistance (R_{rec}) as a function of potential, as shown in Figure 5.

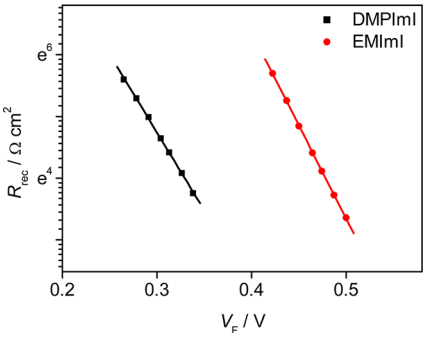

Figure 5. Charge transfer resistance as a function of quasi-Fermi level voltage. The solid lines are fittings to eq 5.

On the basis of β–recombination model,[23] R_{rec} derived from EIS can be expressed as

$$R_{rec} = \frac{K_B T}{q\beta J_0} \exp\left(\frac{-q\beta V_F}{K_B T}\right) = \frac{K_B T}{q\beta J_{0k}} \exp\left(\beta \frac{E_c - E_{redox}}{K_B T}\right) \exp\left(\frac{-q\beta V_F}{K_B T}\right) \quad (5)$$

Fitting the data in Figure 5 to eq 5 gives the values for J_0, J_{0k}, and β as listed in Table 1. According to the slopes displayed in Figure 5, the β factor for EMImI is larger than that for DMPImI. Although EMImI yields a higher J_{0k} than DMPImI, the former generates a lower J_0 due to its higher CB edge and larger β value according to eq 4. Despite the slower charge recombination rate determined by J_{0k} for DMPImI, it produces a lower V_{oc} than EMImI as the latter induces a higher CB edge (Figure 3). The CB edge for the EMImI case is 205 mV higher than that for the DMPImI case, but the V_{oc} for EMImI is 114 mV higher than that for DMPImM. Therefore, the larger charge recombination rate for the EMImI case reduces the V_{oc} by 91 mV.

Effect on FF. According to the result shown in Table 1, the FF for EMImI is much larger than that for DMPImI. Evidently, the ester group has a remarkable effect on FF. Putting the parameter values (Table 1) into the following expression,

$$J = J_{sc} - J_0(e^{\beta q V_F / K_B T} - 1) \quad (6)$$

simulated $J-V$ curves can be obtained, where calculated FF is 0.70 and 0.79 for DMPImI and EMImI, respectively. The calculated FF is larger than the experimental one (Table 1) for both electrolytes. Particularly, the experimental FF is much lower than the calculated one for DMPImI. The decrease in FF can be attributed to the series resistance (R_{series}) that is the sum of all the resistances producing a loss of the electrochemical potential in the device outside the active layer. The R_{series} values obtained from EIS analysis are 45 and 7 Ω cm^2 for DMPImI and EMImI, respectively. The applied voltage is 0.34 V for DMPImI and 0.49 V for EMImI, near each V_{oc}. As EMImI has much larger conductivity than DMPImI, it is reasonable that the former has a smaller series resistance than the latter. The series resistance can decrease FF due to the potential drop associated to R_{series}. Through correction of applied potential by removing the total series resistance, the corrected $J-V$ curves are obtained and shown in Figure 2. The maximum attainable FF (i.e., internal FF) obtained from the corrected $J-V$ curves is 0.71 and 0.79 (Table 1) for DMPImI and EMImI, respectively. The internal FF is in excellent agreement with the calculated FF for both electrolytes, indicating that the reduction of FF is attributed to the effect of series resistance. The larger the series resistance, the larger the difference between the measured FF and the internal value. The internal FF depends on the V_{oc}/m ratio, where m (= $1/\beta$) is the diode quality factor.[18,24] The larger the V_{oc}/m ratio, the larger the internal FF. As EMImI gives larger V_{oc} and smaller m (larger β) than DMPImI, the internal FF for the former should be larger than that for the latter.

CONCLUSIONS

Introduction of an ester group to the imidazolium ring affects solar cell performance significantly, when imidazolium iodide mixed with iodine and LiI is used as the solid electrolyte in ssDSSCs. The strong interaction between Li^+ ions with oxygen atom in the ester group reduces the surface concentration of Li^+ ions on the TiO_2 surface. As a consequence, the CB edge of TiO_2 for the EMImI case is much higher than that for the DMPImI case, which compensates for the voltage loss arising from the higher charge recombination rate and contributes to a higher V_{oc} for EMImI as compared to DMPImI. On the one hand, the series resistance for the EMImI case is small due to its high conductivity, resulting in a good FF that is slightly smaller than the internal FF. On the other hand, the series resistance for the DMPImI case is large due to its low conductivity, leading to a poor FF that is much smaller than the internal FF. Overall, the ester-functionalized imidazolium iodide has advantages over the alkyl-functionalized counterpart in terms of solar cell performance when they are applied as solid state electrolytes in ssDSSCs.

AUTHOR INFORMATION

Corresponding Author

*E-mail: zs.wang@fudan.edu.cn. Tel/Fax: +86-21-5163-0345.

Notes

The authors declare no competing financial interest.

ACKNOWLEDGMENTS

We acknowledge the National Basic Research Program (2011CB933302) of China, the National Natural Science Foundation of China (90922004 and 50903020), STCSM (12JC1401500), Shanghai Pujiang Project (11PJ1401700),

Shanghai Leading Academic Discipline Project (B108), and Jiangsu Major Program (BY2010147) for financial support.

REFERENCES

(1) O'Regan, B.; Grätzel, M. *Nature* **1991**, *353*, 737−740.
(2) Wu, Y.; Zhu, W. *Chem. Soc. Rev.* **2013**, *42*, 2039−2058.
(3) Gong, F.; Wang, H.; Xu, X.; Zhou, G.; Wang, Z.-S. *J. Am. Chem. Soc.* **2012**, *134*, 10953−10958.
(4) Wang, H.; Feng, Q.; Gong, F.; Li, Y.; Zhou, G.; Wang, Z.-S. *J. Mater. Chem. A* **2013**, *1*, 97−104.
(5) Zhu, W.; Wu, Y.; Wang, S.; Li, W.; Li, X.; Chen, J.; Wang, Z.-S.; Tian, H. *Adv. Funct. Mater.* **2011**, *21*, 756−763.
(6) Cui, Y.; Wu, Y.; Lu, X.; Zhang, X.; Zhou, G.; Miapeh, F. B.; Zhu, W.; Wang, Z.-S. *Chem. Mater.* **2011**, *23*, 4394−4401.
(7) Tian, H.; Jiang, X.; Yu, Z.; Kloo, L.; Hagfeldt, A.; Sun, L. *Angew. Chem., Int. Ed.* **2010**, *49*, 7328−7331.
(8) Yella, A.; Lee, H. W.; Tsao, H. N.; Yi, C.; Chandiran, A. K.; Nazeeruddin, M. K.; Diau, E. W. -G.; Yeh, C. -Y.; Zakeeruddin, M. K.; Grätzel, M. *Science* **2011**, *334*, 629−634.
(9) Bach, U.; Lupo, D.; Comte, P.; Moser, J. E.; Weissörtel, F.; Salbeck, J.; Spreitzer, H.; Grätzel, M. *Nature* **1998**, *395*, 583−585.
(10) Koh, J. K.; Kim, J.; Kim, B.; Kim, J. H.; Kim, E. *Adv. Mater.* **2011**, *23*, 1641−1646.
(11) Wu, J.; Hao, S.; Lan, Z.; Lin, J.; Huang, M.; Huang, Y.; Li, P.; Yin, S.; Sato, T. *J. Am. Chem. Soc.* **2008**, *130*, 11568−11569.
(12) Zhao, Y.; Zhai, J.; He, J. L.; Chen, X.; Chen, L.; Zhang, L. B.; Tian, Y. X.; Jiang, L.; Zhu, D. B. *Chem. Mater.* **2008**, *20*, 6022−6028.
(13) Midya, A.; Xie, Z. B.; Yang, J. X.; Chen, Z. K.; Blackwood, D. J.; Wang, J.; Adams, S.; Loh, K. P. *Chem. Commun.* **2010**, *46*, 2091−2093.
(14) Wang, H.; Zhang, X.; Gong, F.; Zhou, G.; Wang, Z.-S. *Adv. Mater.* **2012**, *24*, 121−124.
(15) Koumura, N.; Wang, Z.-S.; Mori, S.; Miyashita, M.; Suzuki, E.; Hara, K. *J. Am. Chem. Soc.* **2006**, *128*, 14256−14257.
(16) Wang, Z.-S.; Koumura, N.; Cui, Y.; Takahashi, M.; Sekiguchi, H.; Mori, A.; Kubo, T.; Furube, A.; Hara, K. *Chem. Mater.* **2008**, *20*, 3993−4003.
(17) Wang, Z.-S.; Kawauchi, H.; Kashima, T.; Arakawa, H. *Coord. Chem. Rev.* **2004**, *248*, 1381−1389.
(18) Fabregat-Santiago, F.; Garcia-Belmonte, G.; Mora-Seró, I.; Bisquert, J. *Phys. Chem. Chem. Phys.* **2011**, *13*, 9083−9118.
(19) Wang, Q.; Ito, S.; Gratzel, M.; Fabregat-Santiago, F.; Mora-Sero, I.; Bisquert, J.; Bessho, T.; Imai, H. *J. Phys. Chem. B* **2006**, *110*, 25210−25221.
(20) Redmond, G.; Fitzmaurice, D. *J. Phys. Chem.* **1993**, *97*, 1426−1430.
(21) van de Lagemaat, J.; Park, N.-G.; Frank, A. J. *J. Phys. Chem. B* **2000**, *104*, 2044−2052.
(22) Bertoluzzi, L.; Ma, S. *Phys. Chem. Chem. Phys.* **2013**, *15*, 4283−4285.
(23) Bisquert, J.; Mora-Seró, I. *J. Phys. Chem. Lett.* **2010**, *1*, 450−456.
(24) Zhang, X.; Wang, S.-T.; Wang, Z.-S. *Appl. Phys. Lett.* **2011**, *99*, 113503: 1−3.